Universal Δ_{max}/T_c in Fe-based superconductors

Siddhant Panda and P. J. Hirschfeld
Department of Physics, University of Florida, Gainesville, Florida 32611, USA

(Received 14 June 2023; revised 7 March 2024; accepted 13 March 2024; published 2 May 2024)

Iron-based superconductors display a large degree of variability in electronic structure at the Fermi surface, resulting in superconducting gap structures, T_c's, and other properties that vary considerably from family to family. Recently, it was noted that across many different families of Fe-based systems, the ratio Δ_{max}/T_c is found to be quasiuniversal with a large value of ∼3.5 compared to the one-band BCS weak-coupling result of 1.76. Here, Δ_{max} is the measured maximum gap across the Fermi surface. This remarkable fact was attributed to strong-coupling effects arising from Hund's metal physics. Here, we perform a "high-throughput" scan across band masses, Fermi energies, and interaction parameters in a weak-coupling Suhl-Matthias-Walker model. We find that unexpectedly large values of Δ_{max}/T_c can be achieved within weak coupling, and that quasiuniversal behavior similar to experiment emerges for those systems where interband interactions dominate intraband ones. However, within the current framework, a large mass contrast between bands is required.

DOI: 10.1103/PhysRevB.109.174504

I. INTRODUCTION

Iron-based superconductors have fascinated the superconductivity community for more than a decade. Originally hailed after their discovery in 2008 [1] as a second class of high-temperature superconductors similar to the cuprates, it was quickly realized that they display a much richer variability of superconducting behavior, due to their multiband, multiorbital character [2]. It is widely believed these Fe-based superconductors (FeSC) are unconventional, i.e., that pairing is driven by repulsive interactions [3]. Unlike cuprates, where a d wave pair state is realized, most iron-based materials are thought to pair in a dominant s-wave state, with different order parameter signs on different bands [4,5]. In addition, experiments show that significant gap anisotropy exists in some materials, including those with gap nodes. Within the usual spin fluctuation theory, this gap structure is driven by several features of the effective interaction, but in particular by the distribution of orbital weights on each Fermi-surface sheet [6–8].

In addition to strongly differing low-temperature gap sizes and structures, the FeSC display a wide range of superconducting transition temperatures, from a few degrees Kelvin up to ∼70 K in monolayer FeSe grown on $SrTiO_3$. Variations in the overall strength of the superconductivity across this family are generally attributed to Fermi-surface features [6–11] such as the number, size, and d-orbital content of the small Fermi-surface pockets around the high-symmetry points of the Brillouin zone, degree of nesting of the pockets, and Fermi velocities. Bare effective Coulomb interactions also vary substantially from material to material [12]. While the phase diagrams of Fe-based systems have some commonalities, there are examples of good superconductors in this class that do not share them. For example, unlike the "canonical" phase diagram where superconductivity evolves via chemical doping from a magnetic parent compound, neither FeSe nor LiFeAs have long-range magnetism at ambient pressure, and require no chemical doping to become superconductors [3].

Thus an apparent overall lack of universality in the properties of the Fe-based systems themselves hinders the search for the underlying, presumed universal physical mechanism of superconductivity. Recently, however, it was pointed out by Miao *et al.* [13] that a sizable number of superconducting Fe-based materials, from very weak to very strong superconductors, have at least one item in common: a quite large value, of roughly 3.5, of the ratio of the maximum $T \to 0$ gap on the Fermi surface, Δ_{max}, to T_c. To show this, values of the ratio Δ_{max}/T_c for 16 materials with widely varying T_c's were compiled from reported angle-resolved photoemission (ARPES) data. In BCS theory for conventional superconductors, this number Δ/T_c is 1.76, and is indeed referred to as a "universal ratio" that emerges from the theory. Of course, it is well known that both strong-coupling effects beyond BCS [14] and gap anisotropy [15] can increase this ratio. Lead (Pb), for example, has a ratio Δ/T_c of about 2.25, and underdoped to optimally doped cuprates have quite large ratios as well [16]. But it is less the size of the ratio that is remarkable in the Fe-based materials, than the apparent universality in a class of superconductors where so much is understood to depend on the details of the electronic structure.

Lee *et al.* [17] approached the problem in terms of a model reflecting Hund's metal physics, including interactions mediated by nearly localized high-energy spin modes. These authors did not attempt to show that universality of the ratio would emerge from models reflecting the degree of variability in the electronic structure of the Fe-based materials. Instead, they studied the so-called "γ model" of a *one-band* superconductor with singular power-law interactions described by a susceptibility $\chi \sim \Omega^{-\gamma}$, and showed that Δ_{max}/T_c could be increased substantially above the BCS value, and agreed with the Miao *et al.* value when $\gamma = 1.2$. Since this behavior is close to the observed behavior γ of Fe-based superconductors at high energies, they suggested that the observed quite large

value of $\Delta_{\max}/T_c$ was due to the physics of a Hund's metal. Within the framework employed, they showed that large gap values were possible, but no real notion of a $\Delta_{\max}/T_c$ robust against system details emerged from these calculations.

Here, we take a quite different approach, arguing that the large $\Delta_{\max}/T_c$ ratio of $\sim$3.5 may in fact be most naturally explained in the framework of a simple multiband weak-coupling theory. By weak coupling, we mean that the interactions within and among bands are assumed much smaller than the relevant Fermi energies and the energies of the pairing bosons. We show, within a simple Suhl-Matthias-Walker (SMW) ansatz of constant pairing interactions in band space [18], that values of $\Delta_{\max}/T_c$ cluster close to a universal value characteristic of the effective mass ratio between the two bands of the model, *provided* the pairing is dominantly interband in nature. This occurs independent of band parameters and other system details. While analytical solutions to this model exist [19,20], the full analytical solution is rather complicated, and our conclusions do not appear to be trivial to extract from it. We therefore exhibit the numerical results, both because we can present our discussion in such a way as to give the reader an intuitive feel for the solution, and because it contains some data outside the strict weak-coupling range.

The measured value $\approx$3.5 of the universal ratio does not emerge naturally unless a very large band mass ratio is assumed, however. As we show, this is *not* characteristic of the Fe-based superconductors. The result is nonetheless quite striking, and we suggest on this basis that the dominant interband nature of the interactions, assumed in many discussions earlier [2,4,5,21] but rather difficult to prove in practice, is the true essential feature of Fe-based superconductivity. In the discussion section, we propose for more realistic multiorbital models a mechanism that may be analogous to the mass anisotropy in the simple two-band case considered here.

II. MODEL

A. Two-band superconductivity

In contrast to Ref. [17], we explore here under which circumstances a "universal" ratio $\Delta_{\max}/T_c$ might be expected in an ensemble of systems characterized by several bands, coupling constants, masses, etc. We begin with a simple two-band model [18,22] with constant interactions within and between bands. To simulate Fe-based systems, we assume that one is a hole band and the other is an electron band, as shown in Fig. 1, with

$$\epsilon_1(\mathbf{k}) = E_{F1} + \frac{(\mathbf{k}-\mathbf{k}_M)^2}{2m_1}, \tag{1}$$

$$\epsilon_2(\mathbf{k}) = E_{F2} - \frac{k^2}{2m_2}. \tag{2}$$

We have modeled the intraband interactions V_{11} and V_{22}, as well as interband interactions V_{12}, using the λ interaction matrix

$$\begin{bmatrix} \lambda_{11} & \lambda_{12} \\ \lambda_{21} & \lambda_{22} \end{bmatrix} = \begin{bmatrix} m_1 * V_{11} & m_2 * V_{12} \\ m_1 * V_{21} & m_2 * V_{22} \end{bmatrix},$$

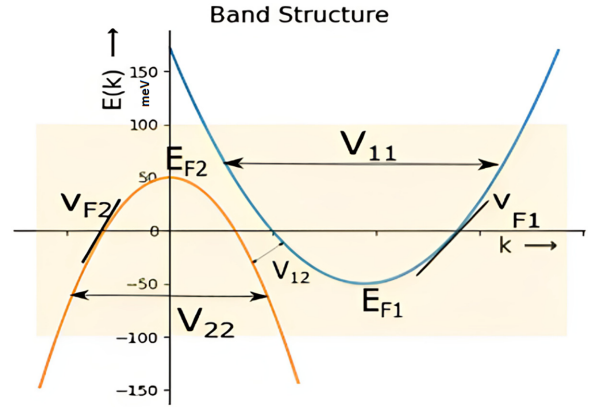

FIG. 1. The band structure of our two-band model for mass ratio 2. $E_{F2} = 50$ meV and $E_{F1} = 50$ meV are the Fermi energies of the two bands. V_{F2} and V_{F1} are the Fermi velocities of the two bands. V_{11}, V_{22}, and V_{12} represent the interactions between the bands. The colored region is the energy cutoff $\omega_d = 100$ meV.

where m_1 and m_2 are the band masses and positive interactions are taken to be attractive. The two-band BCS equations that determines Δ and T_c are

$$\Delta_1 = \lambda_{11}\Delta_1 F_1(\Delta_1, T) + \lambda_{12}\Delta_2 F_2(\Delta_2, T), \tag{3}$$

$$\Delta_2 = \lambda_{22}\Delta_2 F_2(\Delta_2, T) + \lambda_{21}\Delta_1 F_1(\Delta_1, T), \tag{4}$$

and the functions $F_\alpha(\Delta, T)$ for the electron and hole bands $\alpha = 1, 2$ are

$$F_1[\Delta_1, T] = \int_{-E_{F1}}^{\omega_D} d\xi \frac{1}{2\sqrt{\xi^2+\Delta_1^2}} \tanh\left(\frac{\sqrt{\xi^2+\Delta_1^2}}{2T}\right), \tag{5}$$

$$F_2[\Delta_2, T] = \int_{-\omega_D}^{E_{F2}} d\xi \frac{1}{2\sqrt{\xi^2+\Delta_2^2}} \tanh\left(\frac{\sqrt{\xi^2+\Delta_2^2}}{2T}\right), \tag{6}$$

where we have taken the Fermi energies (band extrema) equal $E_{F2} = |E_{F1}| \equiv \epsilon_F$ for simplicity [23], and measured energies relative to the chemical potential μ, $\xi = \epsilon_\alpha(\mathbf{k}) - \mu$ as usual; hence all gaps open below T_c around the fixed chemical potential μ.

We performed a consistency check of our code for mass ratio 2 and different regimes of interband and intraband couplings. We observed from Fig. 2 that when we have no interband coupling, the two Δ behave independently and give two different T_c. But as we progressively keep increasing the interband coupling strength, Δ_1 and Δ_2 converge at the same T_c. Since the mass of band 1 is larger then band 2 initially we have $\Delta_1 > \Delta_2$, but as the interband interaction increases we observe an increase in the Δ_2 value until it finally becomes greater than Δ_1 for an interband larger than the intraband interaction.

$\Delta_{\max}$ is defined to be the maximum of Δ_1, Δ_2 at zero temperature. Note in Miao *et al.* [13], the maximum is also taken over the Fermi surface, but here we adopt an isotropic approximation for simplicity. Although seldom discussed, it is clear that the $\Delta_{\max}/T_c$ ratio can be quite large compared to

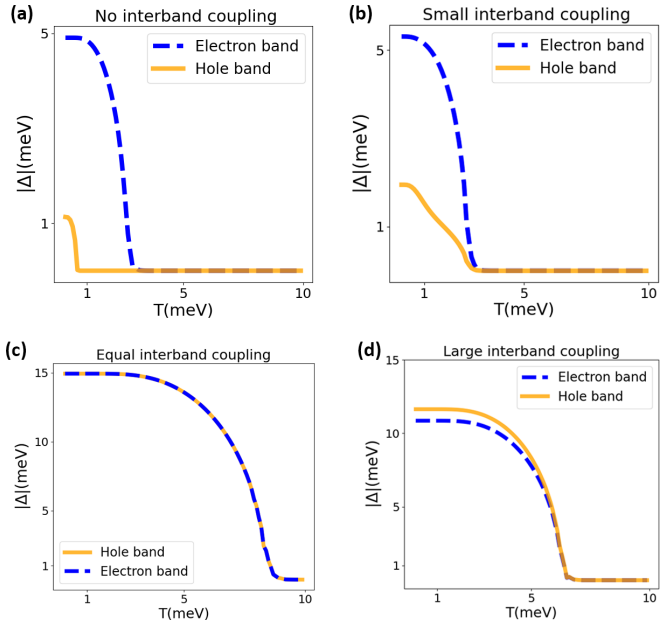

FIG. 2. $|\Delta|$ vs T in various regimes of interband vs intraband pairing with mass ratio 2. (a) $\lambda_{11} = 1.43$ $\lambda_{12/21} = 0$; (b) $\lambda_{11} = 1.43$ and $\lambda_{21} = 0.143$; (c) $\lambda_{11} = \lambda_{21} = 1.43$; (d) $\lambda_{11} = 1.14$ and $\lambda_{21} = 1.43$. For all cases shown, $\lambda_{22} = 2\lambda_{11}$ and $\lambda_{12} = 2\lambda_{21}$.

1.76, generally forcing the minimum gap ratio $\Delta_{\min}/T_c$ at the same time to be considerably smaller.

To differentiate between the different regimes of inter- versus intraband interactions we define a logarithmic quantity

$$\beta = \log \frac{\lambda_{12} + \lambda_{21}}{\lambda_{11} + \lambda_{22}},$$

which parametrizes the degree of interband pairing. $\beta \to \infty$ is pure interband pairing, while $\beta \to -\infty$ is pure intraband pairing.

B. "High-throughput" approach

In a materials class with many different members with quite different electronic structures, it is an appropriate starting point to assume them to have random values of the parameters determining $\Delta_{\max}$ and T_c within reasonable physical ranges. First, we consider a uniform probability distribution of the most important such parameters, namely the individual interaction matrix elements λ_{ij}, as shown in Fig. 3(a). We have divided our study into three regimes based on the values of the elements of the interaction matrix to help identify the qualitative underlying physics. These include three ranges of β identified in the figure by their color coding, strong interband coupling $\beta > 1$ (green), weak interband coupling $\beta < 0$ (blue), and comparable interband and intraband coupling $0 < \beta < 1$ (orange).

Figure 3(a) shows that our distribution is indeed uniform, i.e., not biased towards any particular regime of potentials. The way the points are distributed is as follows. There are roughly an equal number of points for $\beta < 0$ and $\beta > 0$ now since the regime for $\beta > 0$ is divided in $\beta > 1$ and $1 > \beta > 0$ the points are further divided between the two regimes. Figure 3(b) shows that such an evaluation gives rise to T_c values which are not in the physical range, therefore when we look at the results of the high-throughput approach for different mass ratios we will focus mainly at the physical values.

Our high-throughput approach then involves solving (4) for T_c and the superconducting gaps for the various different values of λ_{ij}. We repeat the exercise for differing values of the Fermi energies, effective masses, and BCS pairing cutoffs to check what influences the $\Delta_{\max}/T_c$ ratio. The overall coupling strength is adjusted to keep T_c in a reasonable physical range for Fe-based superconductors.

III. RESULTS

In Fig. 3, we show the results of our high-throughput analysis. We consider two different mass ratios, $m_1/m_2 = 3, 10$, and report the value of $\Delta_{\max}/T_c$ for different λ_{ij}. In Fig. 3(b) we show the $\Delta_{\max}/T_c$ values obtained for the full range of λ's shown in Fig. 3(a) for the particular choice $m_1/m_2 = 10$. Points are distributed between the expected asymptotic ratio values: 1.76 for the weak negligible interband coupling case, as discussed above, and a value close to $\sqrt{m_1/m_2} = 3.16$ for the dominant interband coupling. (see Fig. 4 below and the accompanying discussion). All points in between these asymptotes require numerical evaluation. In Figs. 3(c) and 3(d), the distribution of $\Delta_{\max}/T_c$ is shown for two different values of the mass ratios m_1/m_2, 3 and 10. Independent of the value of the mass ratio, we find some common features, namely clustering around the asymptotic values for small β or large β. When the interband and intraband coupling are comparable, $1 > \beta > 0$, the values of $\Delta_{\max}/T_c$ do not cluster and are instead scattered rather uniformly between the two asymptotes. As seen in Fig. 2, in this regime where the inter/intraband interactions are comparable, the two gaps Δ_1 and Δ_2 are close in magnitude and we observe a crossover from $\Delta_1/\Delta_2 > 1$ to $\Delta_1/\Delta_2 < 1$ when the interband becomes larger than the intraband interaction (for mass ratio $m_1/m_2 > 1$).

In order to achieve a large universal value of the $\Delta_{\max}/T_c$ ratio *within the current simplified framework*, it is clear that we must assume that all materials are dominated by interband pairing interactions, $\beta > 1$. In this case, we have a cluster of points near the upper limit for each mass ratio, so the $\Delta_{\max}/T_c$ ratio is constant and larger than the BCS value for all "samples." The interesting observation is that the upper limit increases with an increase in the mass ratio, as shown in Fig. 4, where we compare with the interband-only solution which was obtained by setting the diagonal terms in the interaction matrix to zero. We further include a comparison with the analytic solution obtained from Ref. [20],

$$\frac{2\Delta_1(0)}{T_c} = 3.52e^{A_1}, \quad \frac{2\Delta_2(0)}{T_c} = 3.52e^{A_2},$$

where

$$A_1 = m_2\tau^2 R\ln(\tau^{-1}), \quad A_2 = -m_1 R\ln(\tau^{-1}),$$
$$R = (m_1 + m_2\tau^2)^{-1},$$

and τ is given by

$$\tau = \tfrac{1}{2}\{\lambda_{22} - \lambda_{11} + [(\lambda_{22} - \lambda_{11})^2 + 4\lambda_{12}\lambda_{21}]^{1/2}\}\lambda_{12}^{-1}.$$

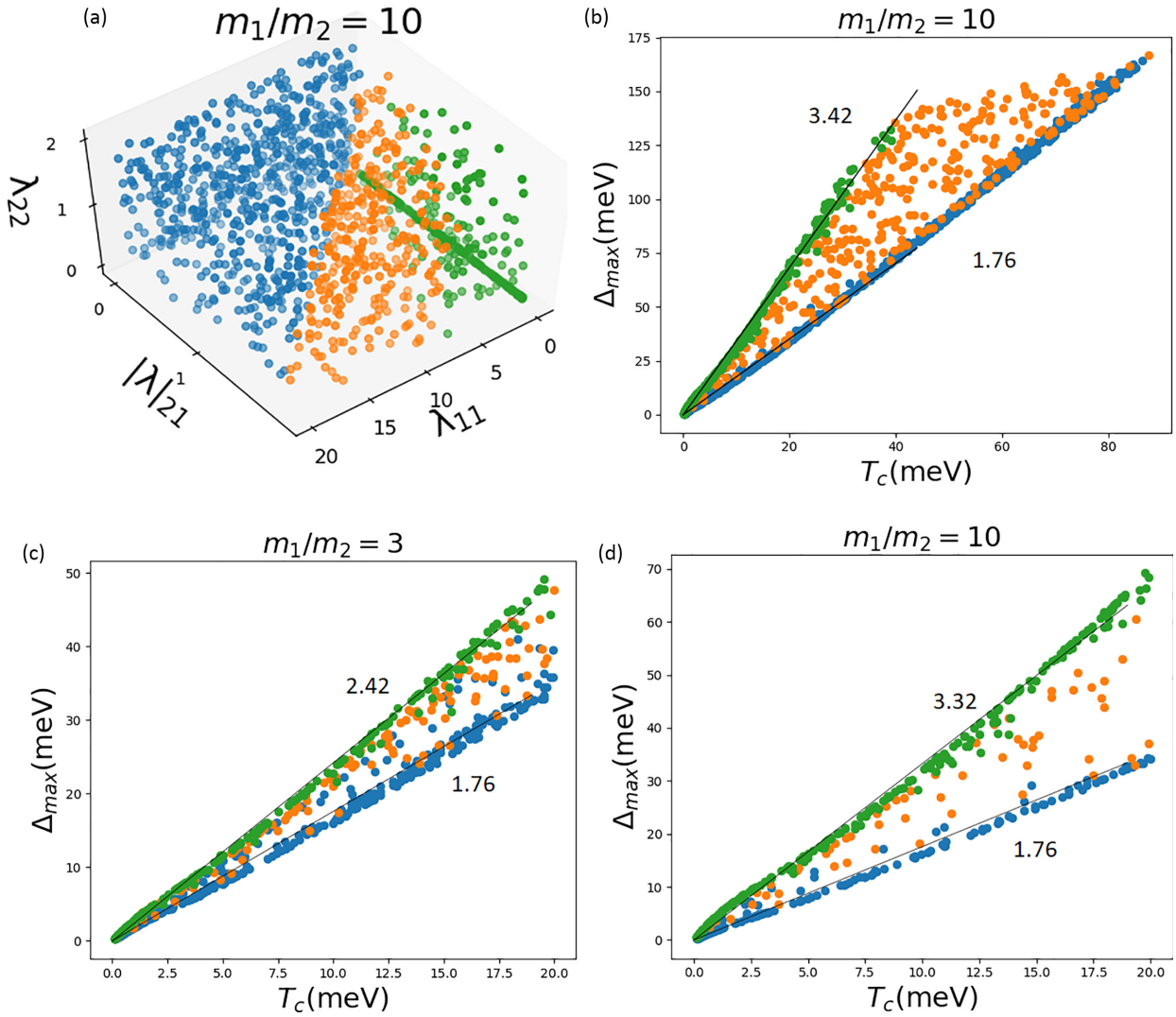

FIG. 3. (a) Uniform distribution of λ_{ij} values used in "high-throughput" search for fixed band mass ratio $m_1/m_2 = 10$. The blue point represents $\beta < 0$, orange points $0 < \beta < 1$, and green points are for $\beta > 1$, representing three regimes of interband and intraband potential ratios. (b) Calculated ratio of the maximum gap to critical temperature, $\Delta_{\max}/T_c$ from two-band BCS equations (4), using parameter sets represented in (a). Note the clustering of points around the weak-coupling value 1.76 and strong-coupling value 3.42. (c), (d) Comparison of high-throughput results for two different mass ratios (3 and 10) in the weak-coupling regime. The upper and lower limits of $\Delta_{\max}/T_c$ for large and small β are indicated by thin solid lines with slopes given.

To find the upper asymptote values of $\Delta_{\max}/T_c$ we work in the pure interband limit where λ_{11} and λ_{22} are zero. Depending on whether we increase ν_1 or ν_2 in our calculation we will have either Δ_1 and Δ_2 giving us our $\Delta_{\max}$. In our study we increase m_1, hence Δ_2 gives us our $\Delta_{\max}$, and we plotted the expression for $\frac{\Delta_2(0)}{T_c}$ in Fig. 4. This $T = 0$ result is quite similar to the well-known exact result $|\Delta_1/\Delta_2| = \sqrt{m_2/m_1}$ that holds in this limit near T_c [11]. However, it requires a mass ratio near 10 to achieve a $\Delta_{\max}/T_c$ ratio near the observed value of 3.5 [13]. Such large mass differentiations are not observed in Fe-based systems, however. In Table I, we exhibit Fermi velocities on electron and hole bands in common units so that a comparison across materials is straightforward. Maximum values of the mass ratio 2–3 are much more typical than the larger values required within this theory. Furthermore, mass ratios differ substantially from material to material, implying a breakdown of any possible universality that might have been present had all interactions been strongly interband in nature and all systems had a common mass ratio.

Other parameters in the model were found to have much less significant impact on the $\Delta_{\max}/T_c$ ratio. For example, we have considered how these results change when the Fermi energies E_{F1} and E_{F2} are varied. We find that the values of $\Delta_{\max}$ and T_c change but the ratio of $\Delta_{\max}/T_c$ does not. The same was true for changes in the energy cutoff. As expected in the weak-coupling limit, changes in the cutoff changed the values of $\Delta_{\max}$ and T_c, but the ratio remained approximately the same for a given mass ratio.

IV. DISCUSSION

We have considered the effect of varying the most common physical quantities thought to influence a superconductor's

TABLE I. Fermi velocities (meVÅ) of electron and hole bands evaluated from ARPES data of different iron-based superconductors. The average mass ratio and the maximum mass ratio were evaluated by the ratio of electron and hole Fermi velocity.

Material	Hole band	Electron band	Average ratio	Max ratio
$FeTe_{0.55}$ $Se_{0.45}$ [28]	95.54, 143.312	N/A	N/A	N/A
$Fe_{1+y}Se_xTe_{1-x}$ [29]	166.66, 166.66, 125	N/A	N/A	N/A
LiFeAs [30]	31.85, 127.38, 0	127.38, 95.54	1.4	4
$Ba_{0.1}K_{0.9}Fe_2As_2$ [31]	84.92, 99.04, 113.23	N/A	N/A	N/A
KFe_2As_2 [32]	60.51, 67.2	37.26, 34.6	1.7	1.94
$NaFe_{0.95}Co_{0.05}$ [33]	24.06	34.4, 80.19	2.38	3.33
$BaFe_2As_2$ [34]	56.78, 113.56	115	1.35	2.02
$BaFeRu_{0.35}As$ [34]	248.4, 248.4	344.9, 172.45	1.04	1.39

critical temperature and gap function [3], in the hopes of understanding if there is a natural explanation for the apparent "universality" of Δ_{max}/T_c throughout the Fe-based family of materials. The model considered here is obviously a vastly oversimplified description of these systems. To name a few clear limitations, we have neglected the dynamics, momentum anisotropy, and orbital dependence of the interaction matrix, self-energy, and vertex correction effects beyond BCS, the correct orbital-dependent electronic structure, spin-orbit coupling, etc. Among these various limitations, let us single out the gap anisotropy for special attention, since it is well known that many of the Fe-based superconductors, including those analyzed by Miao *et al.* [13], are extremely anisotropic, with accidental or symmetry-enforced gap nodes, while others are fully gapped. For some fixed interaction strength, making the gap more anisotropic enhances Δ_{max}/T_c [15,24], suggesting naively that such variability should lead immediately to a breakdown in Δ_{max}/T_c universality. On the other hand, such anisotropy is generally driven by variations in orbital content around the Fermi surface [6], not included in the present approach. So it is not completely implausible that some more general measure of superconducting "fitness" [25,26] including orbital degrees of freedom might preserve the quantity Δ_{max}/T_c despite the apparent large variability of the anisotropy of the interaction across the Fe-based materials.

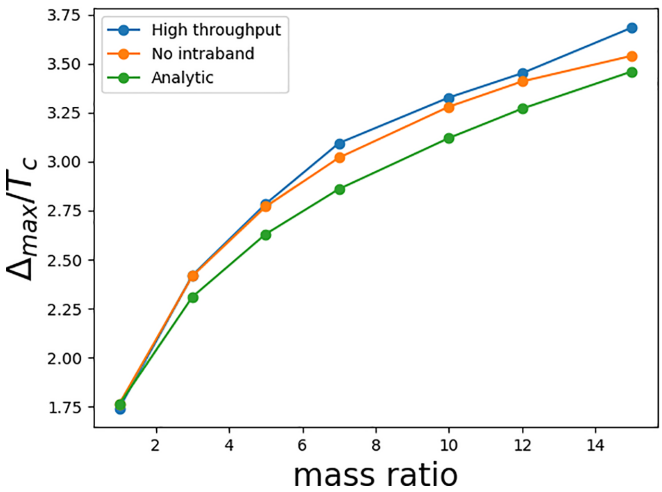

FIG. 4. We compare the Δ_{max}/T_c ratios using our high-throughput approach averaged over the $\beta > 1$ regime, the exact solution for zero intraband coupling $V_{11} = V_{22} = 0$, and the analytic solution from Ref. [20].

It is therefore tempting to speculate that it is the failure to include orbitals and their differentiated electronic correlations in the Fe-based systems which is the principal deficiency of the current model. As has been pointed out in many places, Hund's metal correlations drive a strong asymmetry between d_{xy} and d_{xz}/d_{yz} correlations, e.g., effective masses, a trend observed in nearly all the Fe-based materials [27]. It seems plausible that the "universal" correlation physics of the $d_{xy} - d_{xz/yz}$ splitting may play the role of the mass ratio in this simple model. Investigations of this intriguing hypothesis are in progress.

As a final sanity check, it is useful to compare the current analysis to the more familiar case of MgB_2, to which the two-band model has often been applied [35]. This canonical diboride superconductor with $T_c = 39$ K is generally considered to be an intraband-dominated multiband system with two main gaps driven by the electron-phonon interaction [36]. The average large gap in the system is empirically about 7 meV. Experiments do not to our knowledge give reliable evidence for the gap *anisotropy* , but from EPW calculations [37] the spread in the large gap value over the Fermi surface is ± 0.5 meV [38] giving Δ_{max}/T_c of about 2.2, with the (largest) effective mass ratios from de Haas–van Alphen measurements of about 3.5 [39]. This is roughly consistent with small β values of Δ_{max}/T_c obtained from our simple model [see, e.g., Fig. 3(c)]. Clearly, the claimed Fe-based superconductor universal value of Δ_{max}/T_c of 3.5 represents a new kind of multiband superconducting physics compared to MgB_2, and we have suggested that—up to a point—our model indeed reproduces a universal ratio provided all systems are indeed in the interband-dominated $\beta \gg 1$ limit. The missing link within this framework to obtain actual agreement with the measured *value* $\Delta_{max}/T_c \simeq 3.5$ ratio is a large $[O(10)]$ effective mass ratio between bands, which is not empirically found in the Fe-based systems (Table I).

V. CONCLUSIONS

To investigate the possible existence of the universality of the ratio Δ_{max}/T_c in iron-based superconductors as claimed by Miao *et al* . [13], we solved the weak-coupling two-band equations of superconductivity in a high-throughput approach where the interaction parameters Λ_{ij}, Fermi energies, and masses of electron and hole bands were varied over large but

physical ranges of parameters, and the maximum gap and T_c were determined. We found that for a given mass ratio there is a distribution of $\Delta_{\max}/T_c$ values between the BCS value (1.76) and an upper limit which depends on the mass ratio between electron and hole bands. Although the various parameters are distributed uniformly, there is substantial clustering about the two lines which correspond to the intraband- and interband-dominated limits. In the intermediate regime we have a scatter for many different values. The upper (interband-interaction-dominated) limit increases with increasing mass ratio according to the expected square-root behavior. The conclusion that strong interband pairing may be required to explain the experimental finding is not entirely unexpected, as the usual spin-fluctuation pairing interaction is peaked at $\mathbf{q} = (\pi, 0)$, thereby coupling electron and hole pockets in Fe-based systems. However, we find that the two-band weak-coupling model does *not* display a universal $\Delta_{\max}/T_c$ value, simply because the effective mass ratio observed in ARPES experiments on Fe-based superconductors is not universal. Based on the systematics of the simple two-band case, however, we proposed a study including electronic correlations that may represent a promising way forward.

ACKNOWLEDGMENTS

P.J.H. is grateful to G. Kotliar for bringing Ref. [13] to his attention. The authors thank L. Fanfarillo, V. Kogan, and R. Prozorov for useful discussions. S.P. and P.J.H. were supported by the U.S. Department of Energy under Grant No. DE-FG02-05ER46236.

[1] Y. Kamihara, T. Watanabe, M. Hirano, and H. Hosono, Iron-based layered superconductor La[$O_{1-x}F_x$]FeAs ($x = 0.05$–0.12) with $T_c = 26$ K, J. Am. Chem. Soc. **130**, 3296 (2008).

[2] P. J. Hirschfeld, Using gap symmetry and structure to reveal the pairing mechanism in Fe-based superconductors, C. R. Phys. **17**, 197 (2016).

[3] R. M. Fernandes, A. I. Coldea, H. Ding, I. R. Fisher, P. J. Hirschfeld, and G. Kotliar, Iron pnictides and chalcogenides: A new paradigm for superconductivity, Nature (London) **601**, 35 (2022).

[4] I. I. Mazin, D. J. Singh, M. D. Johannes, and M. H. Du, Unconventional superconductivity with a sign reversal in the order parameter of $LaFeAsO_{1-x}F_x$, Phys. Rev. Lett. **101**, 057003 (2008).

[5] K. Kuroki, S. Onari, R. Arita, H. Usui, Y. Tanaka, H. Kontani, and H. Aoki, Unconventional pairing originating from the disconnected Fermi surfaces of superconducting $LaFeAsO_{1-x}F_x$, Phys. Rev. Lett. **101**, 087004 (2008).

[6] T. A. Maier, S. Graser, D. J. Scalapino, and P. J. Hirschfeld, Origin of gap anisotropy in spin fluctuation models of the iron pnictides, Phys. Rev. B **79**, 224510 (2009).

[7] J. Zhang, R. Sknepnek, R. M. Fernandes, and J. Schmalian, Orbital coupling and superconductivity in the iron pnictides, Phys. Rev. B **79**, 220502(R) (2009).

[8] R. Fernández-Martín, M. J. Calderón, L. Fanfarillo, and B. Valenzuela, The role of orbital nesting in the superconductivity of iron-based superconductors, Condens. Matter **6**, 34 (2021).

[9] S. Graser, T. A. Maier, P. J. Hirschfeld, and D. J. Scalapino, Near-degeneracy of several pairing channels in multiorbital models for the Fe pnictides, New J. Phys. **11**, 025016 (2009).

[10] H. Ikeda, R. Arita, and J. Kuneš, Phase diagram and gap anisotropy in iron-pnictide superconductors, Phys. Rev. B **81**, 054502 (2010).

[11] P. J. Hirschfeld, M. M. Korshunov, and I. I. Mazin, Gap symmetry and structure of Fe-based superconductors, Rep. Prog. Phys. **74**, 124508 (2011).

[12] T. Miyake, K. Nakamura, R. Arita, and M. Imada, Comparison of *ab initio* low-energy models for LaFePO, LaFeAsO, $BaFe_2As_2$, LiFeAs, FeSe, and FeTe: Electron correlation and covalency, J. Phys. Soc. Jpn. **79**, 044705 (2010).

[13] H. Miao, W. H. Brito, Z. P. Yin, R. D. Zhong, G. D. Gu, P. D. Johnson, M. P. M. Dean, S. Choi, G. Kotliar, W. Ku, X. C. Wang, C. Q. Jin, S.-F. Wu, T. Qian, and H. Ding, Universal $2\Delta_{\max}/k_BT_c$ scaling decoupled from the electronic coherence in iron-based superconductors, Phys. Rev. B **98**, 020502(R) (2018).

[14] J. P. Carbotte, Properties of boson-exchange superconductors, Rev. Mod. Phys. **62**, 1027 (1990).

[15] D. Einzel, Analytic two-fluid description of unconventional superconductivity, J. Low Temp. Phys. **131**, 1 (2003).

[16] S.-D. Chen, M. Hashimoto, Y. He, D. Song, K.-J. Xu, J.-F. He, T. P. Devereaux, H. Eisaki, D.-H. Lu, J. Zaanen, and Z.-X. Shen, Incoherent strange metal sharply bounded by a critical doping in Bi2212, Science **366**, 1099 (2019).

[17] T.-H. Lee, A. V. Chubukov, H. Miao, and G. Kotliar, Pairing mechanism in Hund's metal superconductors and the universality of the superconducting gap to critical temperature ratio, Phys. Rev. Lett. **121**, 187003 (2018).

[18] H. Suhl, B. T. Matthias, and L. R. Walker, Bardeen-Cooper-Schrieffer theory of superconductivity in the case of overlapping bands, Phys. Rev. Lett. **3**, 552 (1959).

[19] L. P. Gor'kov, The superconductor-exitonic dielectric phase transition in a semimetal, Zh. Eksp. Teor. Fiz. **63**, 1059 (1972) [Sov. Phys. - JETP **36**, 556 (1973)].

[20] V. Kresin and S. Wolf, Multigap structure in the cuprates, Physica C: Superconductivity **169**, 476 (1990).

[21] O. V. Dolgov, I. I. Mazin, D. Parker, and A. A. Golubov, Interband superconductivity: Contrasts between Bardeen-Cooper-Schrieffer and Eliashberg theories, Phys. Rev. B **79**, 060502(R) (2009).

[22] V. A. Moskalenko, Superconductivity of metals with overlapping of energetic bands, Fiz. Met. Metalloved. **8**, 503 (1959).

[23] We verified that results are generally insensitive to changes in the high-energy electronic structure.

[24] V. G. Kogan and R. Prozorov, Temperature dependence of London penetration depth anisotropy in superconductors with anisotropic order parameters, Phys. Rev. B **103**, 054502 (2021).

[25] A. Ramires and M. Sigrist, Identifying detrimental effects for multiorbital superconductivity: Application to Sr_2RuO_4, Phys. Rev. B **94**, 104501 (2016).

[26] A. Ramires, D. F. Agterberg, and M. Sigrist, Tailoring T_c by symmetry principles: The concept of superconducting fitness, Phys. Rev. B **98**, 024501 (2018).

[27] M. Yi, Y. Zhang, Z.-X. Shen, and D. Lu, Role of the orbital degree of freedom in iron-based superconductors, npj Quantum Mater. **2**, 57 (2017).

[28] H. Miao, P. Richard, Y. Tanaka, K. Nakayama, T. Qian, K. Umezawa, T. Sato, Y.-M. Xu, Y. B. Shi, N. Xu, X.-P. Wang, P. Zhang, H.-B. Yang, Z.-J. Xu, J. S. Wen, G.-D. Gu, X. Dai, J.-P. Hu, T. Takahashi, and H. Ding, Isotropic superconducting gaps with enhanced pairing on electron Fermi surfaces in $FeTe_{0.55}Se_{0.45}$, Phys. Rev. B **85**, 094506 (2012).

[29] S. Rinott, K. B. Chashka, A. Ribak, E. D. L. Rienks, A. Taleb-Ibrahimi, P. L. Fevre, F. Bertran, M. Randeria, and A. Kanigel, Tuning across the BCS-BEC crossover in the multiband superconductor $Fe_{1+y}Se_xTe_{1-x}$: An angle-resolved photoemission study, Sci. Adv. **3**, e1602372 (2017).

[30] H. Miao, Z. P. Yin, S. F. Wu, J. M. Li, J. Ma, B.-Q. Lv, X. P. Wang, T. Qian, P. Richard, L.-Y. Xing, X.-C. Wang, C. Q. Jin, K. Haule, G. Kotliar, and H. Ding, Orbital-differentiated coherence-incoherence crossover identified by photoemission spectroscopy in LiFeAs, Phys. Rev. B **94**, 201109(R) (2016).

[31] N. Xu, P. Richard, X. Shi, A. van Roekeghem, T. Qian, E. Razzoli, E. Rienks, G.-F. Chen, E. Ieki, K. Nakayama, T. Sato, T. Takahashi, M. Shi, and H. Ding, Possible nodal superconducting gap and Lifshitz transition in heavily hole-doped $Ba_{0.1}K_{0.9}Fe_2As_2$, Phys. Rev. B **88**, 220508(R) (2013).

[32] T. Yoshida, S.-I. Ideta, I. Nishi, A. Fujimori, M. Yi, R. Moore, S.-K. Mo, D. Lu, Z.-X. Shen, Z. Hussain, K. Kihou, P. Shirage, H. Kito, C.-H. Lee, A. Iyo, H. Eisaki, and H. Harima, Orbital character and electron correlation effects on two- and three-dimensional Fermi surfaces in KFe_2As_2 revealed by angle-resolved photoemission spectroscopy, Front. Phys. **2**, 17 (2014).

[33] Z.-H. Liu, P. Richard, K. Nakayama, G.-F. Chen, S. Dong, J.-B. He, D.-M. Wang, T.-L. Xia, K. Umezawa, T. Kawahara, S. Souma, T. Sato, T. Takahashi, T. Qian, Y. Huang, N. Xu, Y. Shi, H. Ding, and S.-C. Wang, Unconventional superconducting gap in $NaFe_{0.95}Co_{0.05}As$ observed by angle-resolved photoemission spectroscopy, Phys. Rev. B **84**, 064519 (2011).

[34] V. Brouet, F. Rullier-Albenque, M. Marsi, B. Mansart, M. Aichhorn, S. Biermann, J. Faure, L. Perfetti, A. Taleb-Ibrahimi, P. Le Fèvre, F. Bertran, A. Forget, and D. Colson, Significant reduction of electronic correlations upon isovalent Ru substitution of $BaFe_2As_2$, Phys. Rev. Lett. **105**, 087001 (2010).

[35] H. Kim, K. Cho, M. A. Tanatar, V. Taufour, S. K. Kim, S. L. Bud'ko, P. C. Canfield, V. G. Kogan, and R. Prozorov, Self-consistent two-gap description of MgB_2 superconductor, Symmetry **11**, 1012 (2019).

[36] S. L. Bud'ko and P. C. Canfield, Superconductivity of magnesium diboride, Physica C: Supercond. Appl. **514**, 142 (2015).

[37] E. R. Margine and F. Giustino, Anisotropic Migdal-Eliashberg theory using Wannier functions, Phys. Rev. B **87**, 024505 (2013).

[38] The overall pairing scale in these calculations [37] is well known to be of order 20% too high, but the relative measure of the gap anisotropy should be quite accurate.

[39] S. Elgazzar, P. Oppeneer, S.-L. Drechsler, R. Hayn, and H. Rosner, Calculated de Haas–van Alphen data and plasma frequencies of MgB_2 and TaB_2, Solid State Commun. **121**, 99 (2002).